JBC ARTICLE

Ubiquitination of interleukin-1α is associated with increased pro-inflammatory polarization of murine macrophages deficient in the E3 ligase ITCH

Received for publication, May 12, 2020, and in revised form, June 21, 2020 Published, Papers in Press, June 25, 2020, DOI 10.1074/jbc.RA120.014298

Xi Lin[1], **Hengwei Zhang**[1], **Brendan F. Boyce**[1,2], **and Lianping Xing**[1,2,*]

From the [1]*Department of Pathology and Laboratory Medicine and* [2]*Center for Musculoskeletal Research, University of Rochester Medical Center, Rochester, New York, USA*

Edited by George N. DeMartino

Macrophages play critical roles in homeostasis and inflammation. Macrophage polarization to either a pro-inflammatory or anti-inflammatory status is controlled by activating inflammatory signaling pathways. Ubiquitination is a post-translational modification that regulates these inflammatory signaling pathways. However, the influence of protein ubiquitination on macrophage polarization has not been well studied. We hypothesized that the ubiquitination status of key proteins in inflammatory pathways contributes to macrophage polarization, which is regulated by itchy E3 ubiquitin ligase (ITCH), a negative regulator of inflammation. Using ubiquitin proteomics, we found that ubiquitination profiles are different among polarized murine macrophage subsets. Interestingly, interleukin-1α (IL-1α), an important pro-inflammatory mediator, was specifically ubiquitinated in lipopolysaccharide-induced pro-inflammatory macrophages, which was enhanced in ITCH-deficient macrophages. The ITCH-deficient macrophages had increased levels of the mature form of IL-1α and exhibited pro-inflammatory polarization, and reduced deubiquitination of IL-1α protein. Finally, IL-1α neutralization attenuated pro-inflammatory polarization of the ITCH-deficient macrophages. In conclusion, ubiquitination of IL-1α is associated with increased pro-inflammatory polarization of macrophages deficient in the E3 ligase ITCH.

Inflammation is the host's response to exogenous pathogen invasion or endogenous signals such as damaged cells. Inflammation is critical for tissue repair but can also lead to local or systemic tissue damage if unchecked (1). Macrophages are plastic immune cells necessary for maintaining homeostasis and controlling inflammation (2). Once activated, macrophages are polarized into pro-inflammatory or anti-inflammatory macrophages (3, 4). Given the critical role of macrophages in inflammation, it is important to understand the regulation of macrophage polarization to intervene in unrestrained inflammation.

Macrophages survey their milieu for abnormal microenvironmental stimuli through pattern-recognition receptors. Pathogens and environmental challenges activate macrophages and trigger inflammatory pathways such as the archetypical nuclear factor-κB (NF-κB) pathway, resulting in the production of key inflammatory cytokines, including interleukin-1 (IL-1) and tumor necrosis factor (TNF) (2). Cytokines differentially activate macrophages, resulting in macrophage polarization. Pro-inflammatory macrophages are activated by numerous factors, including lipopolysaccharide (LPS) and interferon-γ (IFN-γ) and characterized by increased inducible nitric oxide synthase (iNOS) expression and nitric oxide production, which play a central role in the pathogen-killing inflammatory response. In contrast, anti-inflammatory macrophages are activated by IL-4 and characterized by increased arginase expression to promote ornithine metabolism, which is crucial for cell proliferation and tissue repair (5).

Previous studies linked macrophage activation with the ubiquitination (ub) status of key proteins in inflammatory signal pathways (6). Lysine-48 ub (Lys-48–ub) of the NF-κB inhibitor (IκB), the final checkpoint of the NFκB pathway, leads to IκB degradation and consequent NF-κB–associated inflammation (7). In contrast, TRAF6, an upstream positive regulator of the NF-κB pathway, is modulated by Lys-63–ub, leading to its conformational change and activation (8). However, a comprehensive analysis of ub profiles of polarized macrophages has not been reported. Whether a unique ub signature is associated with individual macrophage subsets is not known.

Ub status of a protein is controlled by both ub and de-ub enzymes. The ub process is catalyzed sequentially by ubiquitin E1, E2, and E3 ligases whereas de-ub is carried out by de-ub enzymes (DUB). ITCH is a well-characterized negative regulator of inflammation that functions as an E3 ligase as well as an adaptor protein of DUB in addition to catalyzing the final step of protein ub (9). ITCH catalyzes the Lys-48–ub of the pro-inflammatory AP-1 and JunB transcription factors, marking them for degradation, and consequently inhibits the expression of downstream cytokines in T cells (10). In contrast, ITCH forms complexes with the DUB enzyme A20 in mouse embryonic fibroblasts, resulting in inflammation inhibition (11). We reported that ITCH interacts with DUB enzyme CYLD to reverse the Lys-63–ub of TRAF6 and down-regulate the NF-κB pathway in osteoclast precursors (12). However, the role of ITCH as a ub modulator in polarized macrophages has not been studied. *Itch* is expressed at low levels at baseline. *Itch* is an NF-κB target-responsive gene, and with pro-inflammatory stimulation such as LPS, the expression of *Itch* is elevated to negatively regulate inflammation (9). Thus, exploring genes and proteins affected in Itch−/− macrophages will improve

This article contains supporting information.

* For correspondence: Lianping Xing, Lianping_xing@urmc.rochester.edu.

our understanding of the negative regulation during sustained inflammation.

IL-1 is an important pro-inflammatory cytokine. IL-1 family cytokines include IL-1α and IL-1β; both bind to the same IL-1 receptor and eventually activates NF-κB signaling to induce inflammation (13). The ub of pro–IL-1β promotes its catalytic processing and subsequent maturation (14). However, how the ub and de-ub regulation of IL-1 affects mac polarization is unknown.

In the current study, we show that quiescent, pro-inflammatory, and anti-inflammatory macrophages have distinct ub profiles and elevated ub of IL-1α in LPS-induced pro-inflammatory macrophages ITCH inhibits inflammatory cytokine IL-1α maturation by promoting the de-ub of pro–IL-1α, thereby negatively regulating LPS–macs pro-inflammatory polarization. Our data indicate that the ub status of key mediators affects macrophage pro-inflammatory polarization, which is regulated by ITCH. Our study provides rationale for modulating protein ub of key regulators in macrophages as an approach to interfere with inflammatory diseases.

Results

The expressional levels of total ubiquitinated proteins are similar in pro-inflammatory and anti-inflammatory macrophages

To test whether protein ub is altered during macrophage polarization, we treated WT BMMs with LPS to induce pro-inflammatory macrophages or IL-4 to induce anti-inflammatory macrophages using the protocol that we have described recently (15, 16) in which iNOS was used as the marker for pro-inflammatory macrophages and CD206 was used as marker for anti-inflammatory macrophages, and PBS-treated cells were used as control. We assessed the expressional levels of total ubiquitinated proteins by Western blot analysis. We validated our cell model by assessing the expression of surface markers and effector genes expression in these cells (Fig. 1, *A* and *B*). Consistent with the literature (17), LPS-treated cells (LPS-macs) were stained positively for iNOS whereas IL-4–treated cells (IL-4–macs) were stained positively for CD206, surface markers for pro-inflammatory and anti-inflammatory macrophages, respectively (Fig. 1*A*). LPS-macrophages had a pro-inflammatory gene expression profile with ~500- to 1000-fold-increases in *IL-1β*, *NOS2*, and *TNF* mRNA levels compared with PBS-macs, whereas IL-4–macs had an anti-inflammatory gene expression profile with a similar -fold increase of *IL10* and *PPARγ* mRNA expression (Fig. 1*B*). Surprisingly, the expressional levels of total ubiquitinated proteins were similar in all three types of macrophages (Fig. 1*C*), suggesting that changes in ub of specific proteins, rather than the total amount of ubiquitinated proteins, may be associated with macrophage polarization.

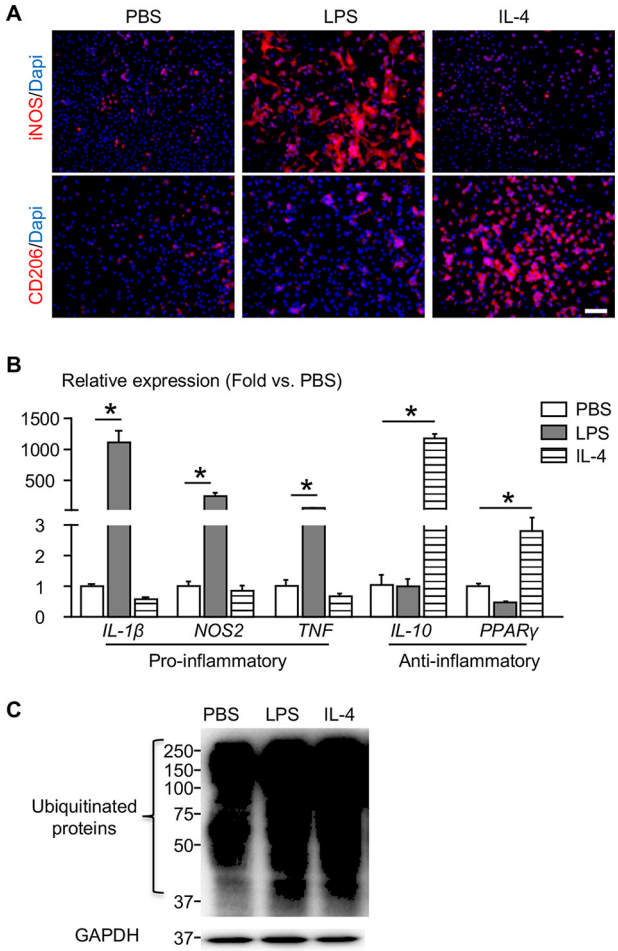

Figure 1. The expressional levels of total ubiquitinated proteins are similar in pro-inflammatory and anti-inflammatory macrophages. BMMs from WT C57BL/6J mice were treated with LPS (100 ng/ml) or IL-4 (100 ng/ml) for 24 h to induce pro-inflammatory and anti-inflammatory macrophages, respectively. PBS-treated cells were used as controls. *A*, representative images show that immunofluorescence-stained cells for iNOS (taken at 10× magnification, *scale bar* = 50 μM), a marker for pro-inflammatory macrophages or CD206, a marker for anti-inflammatory macrophages. $n = 3$ repeats. *B*, relative expression of effector genes of pro- or anti-inflammatory macrophages by qPCR. Values are mean ± S.D. of three wells. -Fold changes of genes were calculated by normalized to actin expression level and then to PBS-macs. Data were analyzed by one-way ANOVA followed by a Tukey test. *, $p < 0.05$. *C*, expression of total ubiquitinated proteins was assessed by Western blot analysis using an anti-ubiquitin antibody. $n = 2$ repeats.

Key proteins of pro-inflammatory polarization are differentially ubiquitinated in LPS-induced macrophages

To identify key regulatory proteins in macrophage polarization, we assessed the ub profiles of LPS-, IL-4–, and PBS-macs (Fig. 2*A*) using the ubiquitin proteomics approach (18). As expected, ub profiles were different among three macrophage subsets; 30, 32, and 14 proteins were differentially ubiquitinated in PBS-, LPS-, and IL-4–macs, respectively (Fig. 2*B* and Table 1 detailed the ubiquitin proteomics findings in Table S1 and PRIDE dataset identifier PXD018743). Among 32 ubiquitinated proteins in pro-inflammatory LPS-macs, iNOS and IL-1α were the fifth and eighth highest ubiquitinated proteins (Fig. 2*C*). Both iNOS and IL-1 proteins undergo posttranslational modification by ub (19, 20). However, how ub of iNOS and IL-1α affects macrophage polarization has not been studied.

ITCH limits pro-inflammatory phenotype and affects the ub status of IL-1α in macrophages

Previous studies reported that the ubiquitin E3 ligase ITCH limits inflammatory responses by negatively regulating LPS-

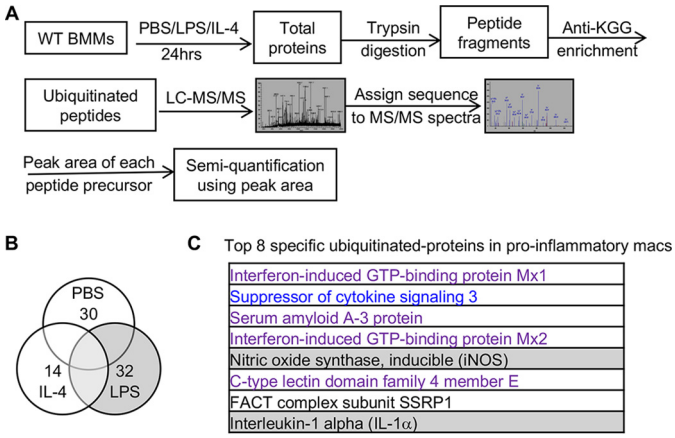

Figure 2. Differentially ubiquitinated proteins in pro-inflammatory and anti-inflammatory macrophages. BMMs were treated as in Fig. 1 except for the addition of MG132 in the last 4 h before cells were harvested. *A*, flowchart of ubiquitin proteomics. *B*, Venn diagram illustrates the distribution of ubiquitinated proteins and selection of highly ubiquitinated proteins specific to each subset of macrophages. *C*, the list of top eight differentially ubiquitinated proteins in pro-inflammatory macrophages.

induced NF-κB activation (11, 12). However, whether ITCH affects ub of iNOS or IL-1α as a molecular mechanism for its anti-inflammatory effect has not been studied. To explore if ITCH mediated the ub of iNOS and IL-1α in macrophages, we utilized ITCH-deficient cells. Compared with WT LPS-macs, Itch−/− LPS-macs had 2-fold increased iNOS signal intensity by immunofluorescence staining (Fig. 3, *A* and *B*). Expression of *NOS2* and *IL1β* mRNA significantly increased 5.44-fold in Itch−/− LPS-macs compared with 1.36-fold in WT LPS-macs (Fig. 3*C*). These data suggest that Itch−/− macrophages are predisposed to pro-inflammatory polarization. To determine whether ITCH negatively regulates pro-inflammatory polarization by mediating ub of IL-1α or iNOS in macrophages, we assessed the ub status of iNOS and IL-1α in macrophages from Itch−/− mice Ubiquitinated iNOS levels were comparable in Itch−/− and WT LPS-macs (4.1 ± 0.9 in Itch−/− *versus* 3.72 ± 0.74 in WT, -fold increase of LPS-macs over WT PBS-macs) (Fig. 4*A*). However, ubiquitinated IL-1α levels were ∼2-fold higher in Itch−/− compared with WT cells (9.27 ± 1.16 in Itch−/− *versus* 4.36 ± 1.05 in WT, -fold increase of LPS-macs over WT PBS-macs) (Fig. 4*B*), indicating that the ub status of IL-1α, but not iNOS, may be regulated by ITCH.

ITCH promotes the de-ub of IL-1α in pro-inflammatory macrophages

Elevated ubiquitinated IL-1α in Itch−/− macrophages (Fig. 4) suggested that ITCH functioned as an adaptor protein for DUB enzymes to remove ubiquitin from IL-1α. To test whether ITCH affected the de-ub of IL-1α, we stimulated macrophages with LPS for 8 h and assessed the levels of ubiquitinated IL-1α 8 h and 16 h after removing LPS from the culture (Fig. 5*A*). We found that ubiquitinated IL-1α proteins were higher in Itch−/− macrophages compared with WT macrophages after LPS removal (-fold increase over PBS: 3.76 ± 1.00 in Itch−/− *versus* 1.24 ± 0.52 in WT cells at 8 h; 1.73 ± 0.45 in Itch−/− *versus* 0.69 ± 0.32 at 16 h) (Fig. 5, *B* and *C*). Furthermore, ubiquitinated

Table 1
Specifically ubiquitinated proteins in PBS-, LPS-, or IL-4–treated macrophages

A. Specific ubiquitinated-proteins in PBS-treated macrophages
RNA polymerase II subunit A C-terminal domain phosphatase
Mitofusin-2
Tyrosine-protein phosphatase nonreceptor type 12
Aspartate aminotransferase, cytoplasmic OS = *Mus musculus*
Protein fem-1 homolog C
NADH dehydrogenase (ubiquinone) 1 beta subcomplex subunit 10
Sorting nexin-30
Platelet-activating factor receptor
H^+/Cl^- exchange transporter 7
Thioredoxin-related transmembrane protein 2
Vacuolar protein sorting-associated protein 13B
Lysosome-associated membrane glycoprotein 1
Protein BANP
Brain-specific angiogenesis inhibitor 1–associated protein 2
RanBP-type and C3HC4-type zinc finger–containing protein 1
Ubiquitin-conjugating enzyme E2 Z
SWI/SNF-related matrix-associated actin-dependent regulator of chromatin subfamily D member 2
Mitogen-activated protein kinase 6
Regulatory-associated protein of mTOR
DNA polymerase δ subunit 3
Band 3 anion transport protein
Suppressor of IKBKE 1
Tyrosine-protein phosphatase nonreceptor type 22
Centromere protein H
Vacuolar protein sorting–associated protein 33B
ATP-dependent DNA helicase Q1
Importin subunit α-7
Protein CLN8
Leucine zipper–like transcriptional regulator 1
Serine/arginine-rich splicing factor 1
B. Specific ubiquitinated-proteins in pro-inflammatory macrophages
Interferon-induced GTP-binding protein M× 1
Suppressor of cytokine signaling 3
Serum amyloid A-3 protein
Interferon-induced GTP-binding protein M× 2
Nitric oxide synthase, inducible
C-type lectin domain family 4 member E
FACT complex subunit SSRP1
Interleukin-1α
Plasminogen activator inhibitor 1 RNA-binding protein
Ryanodine receptor 1
Serine/threonine-protein kinase 11 interacting protein
Peroxisomal membrane protein PMP34
Ubiquitin-conjugating enzyme E2 R1
Metalloreductase STEAP4
Alstrom syndrome protein 1 homolog
CUE domain-containing protein 2
Ganglioside-induced differentiation-associated protein 2
E3 ubiquitin-protein ligase NEURL3
cAMP-specific 3′,5′-cyclic phosphodiesterase 4A
Leukotriene A-4 hydrolase
TCDD-inducible poly (ADP-ribose) polymerase
Dihydrolipoyl dehydrogenase, mitochondrial
Cytosolic acyl CoA thioester hydrolase
Cell division cycle–associated 7–like protein
Translin
Glycerol kinase
Type II inositol 1,4,5-trisphosphate 5-phosphatase
B-cell lymphoma 3 protein homolog
Myomesin-1
Kinetochore-associated protein 1
Band 4.1–like protein 2
Probable ATP-dependent RNA helicase DDX49
C. Specific ubiquitinated-proteins in anti-inflammatory macrophages
60S ribosomal protein L17
Coatomer subunit δ
Glutaminase kidney isoform, mitochondrial
Heterogeneous nuclear ribonucleoprotein A1
E3 ubiquitin-protein ligase AMFR
Mitochondrial import receptor subunit TOM70
1-phosphatidylinositol 3-phosphate 5-kinase
Lupus La protein homolog
Actin-related protein 10
Caspase-6
Structural maintenance of chromosomes protein 4
Cullin-1 OS = *Mus musculus* G*n* = Cul1 PE = 1 SV = 1
AP-3 complex subunit μ-1
Myosin regulatory light chain 2, skeletal muscle isoform

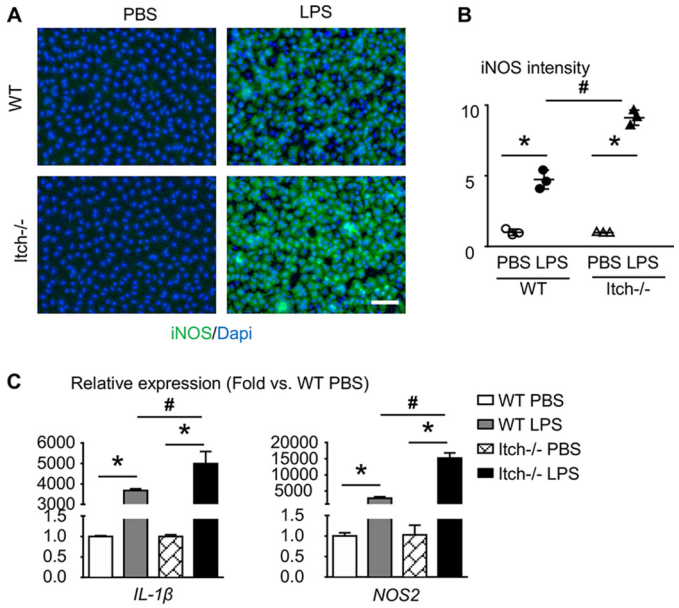

Figure 3. Itch−/− macrophages are more susceptible to pro-inflammatory polarization. BMMs from Itch−/− mice or WT littermate controls were treated with LPS (500 ng/ml) for 24 h to induce pro-inflammatory macrophages. PBS-treated cells were used as controls. *A*, representative images (taken at 10× magnification, *scale bar* = 50 μM) show that immunofluorescence-stained cells for iNOS, a marker for pro-inflammatory macrophages. n= 3 repeats. *B*, iNOS intensity was quantified with ImageJ. Values are the mean ± S.D. of three wells. Data are analyzed with two-way ANOVA followed by Sidak's post hoc test. *, $p < 0.05$ LPS *versus* PBS; #, $p < 0.05$ Itch−/− *versus* WT. *C*, relative expression of *IL-1β* and *NOS2* mRNA by qPCR. Values are mean ± S.D. of three wells. -Fold changes of genes were calculated by normalized to actin expression and then to PBS-treated WT macrophages. Data were analyzed by two-way ANOVA followed by Sidak's post hoc test. *, $p <$ 0.05 LPS-macs *versus* PBS-macs; #, $p < 0.05$ Itch−/− cells *versus* WT cells (only the statistics of the comparison between Itch−/− *versus* WT with the same treatment are shown).

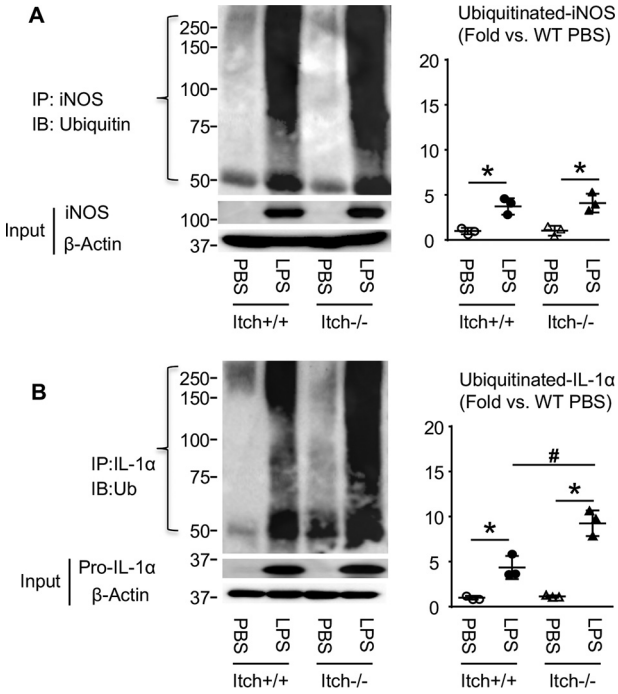

Figure 4. Elevated ubiquitinated IL-1α in Itch−/− pro-inflammatory macrophages. BMMs from Itch−/− mice or WT littermate controls were treated as in Fig. 3. Whole-cell lysates were immunoprecipitated with anti-iNOS or anti–IL-1α antibodies and IP complexes were blotted with an anti-ubiquitin antibody. iNOS and IL-1α protein expression in the input whole lysates were used as controls. The intensity of the ubiquitinated iNOS or IL-1α was quantified with ImageJ as average intensity density × the area of the smeared band. The levels of ubiquitinated proteins were normalized to actin and then to PBS-treated WT samples. *A*, ubiquitinated iNOS was increased in LPS-macs, but is similar between WT and Itch−/− LPS-macs. *B*, ubiquitinated IL-1α was increased in LPS-macs and was further increased in Itch−/− LPS-macs. Data were analyzed with two-way ANOVA followed by Sidak's post hoc test. Values are mean ± S.D. of $n = 3$. *, $p < 0.05$ LPS-macs *versus* PBS-macs; #, $p < 0.05$ Itch−/− cells *versus* WT cells (only the statistics of the comparison between Itch−/− *versus* WT with the same treatment are shown).

IL-1α decreased slower in Itch−/− LPS-macs compared with WT (percentage decrease of ubiquitinated IL-1α during the chase: −1.09 ± 27.59% in Itch−/− *versus* 61.09 ± 12.51% in WT cells at 8 h; 50.43 ± 3.97 in Itch−/− *versus* 78.68 ± 5.70 at 16 h) (Fig. 5*D*). In contrast, the expression of *IL-1α* mRNA was not significantly different between Itch−/− and WT macrophages after removing LPS (Fig. 5*E*), suggesting that higher levels of ubiquitinated IL-1α in Itch−/− macrophages after LPS removal were not because of transcriptional regulation. Because the levels of ubiquitinated IL-1α were higher after LPS removal in macrophage-deficient ITCH, we suspected that ITCH may affect the de-ub process via its adaptor function, *i.e.* ITCH works with DUB enzymes to reduce IL-1α ubiquitination. To test this possibility, we treated LPS-macs 8 h after LPS removal (Fig. 5*B*, *lanes 3* and *7*) with a DUB inhibitor WP1130. WP1130 increased ubiquitinated IL-1α in WT LPS macrophages (Fig. 5*F*, *lane 4 versus lane 3*; (Fig. 5*G*) -fold increase over PBS: 9.78 ± 2.44 in WP1130-treated WT LPS-macs *versus* 3.83 ± 1.04 in vehicle-treated WT LPS-macs) to a similar level to that of Itch−/− macrophages (Fig. 5*F*, *lane 4 versus lane 7*; (Fig. 5*G*) -fold increase over PBS: 9.78 ± 2.44 in WP1130-treated WT LPS-macs *versus* 7.99 ± 1.96 in vehicle-treated Itch−/− LPS-macs). Thus, Itch regulates the ub status of IL-1α by promoting its de-ub process, which can be blocked by ITCH depletion or the DUB inhibition.

Mature form of IL-1α increases in pro-inflammatory macrophage-deficient ITCH

We then studied how reduced IL-1α de-ub contributes to increased pro-inflammatory phenotype in Itch−/− LPS-macs because of the positive correlation between ubiquitinated IL-1α and inflammation (Figs. 3 and 4). We hypothesized that ub promoted the processing of pro–IL-1α, resulting in its maturation. We found that mature form of IL-1α increased ~2-fold in Itch−/− LPS-macs compared with WT cells (-fold increase of LPS-macs over WT PBS-macs: 13.33 ± 2.57 in Itch−/− *versus* 7.98 ± 0.039 in WT cells) (Fig. 6*A*) measured by Western blot analysis based on the different molecular weights of pro– and mature IL-1α. Consistently, secreted IL-1α in the supernatant of Itch−/− LPS-macs was ~2.5-fold higher than WT (-fold increase of LPS-macs over WT PBS-macs: 62.70 ± 4.20 in Itch−/− *versus* 24.75 ± 2.25 in WT cells) (Fig. 6*B*) measured using ELISA that measures soluble IL-1α acquired upon maturation. Because the maturation of pro–IL-1α is chiefly catalyzed by granzyme B (21), it is possible that ITCH depletion increases mature IL-1α by increasing the enzymatic activity of granzyme B. To test this, we assessed granzyme B activity using specific substrate Ac-IETD-AFC. Although granzyme B activity increased after LPS stimulation in both WT and Itch−/− LPS-

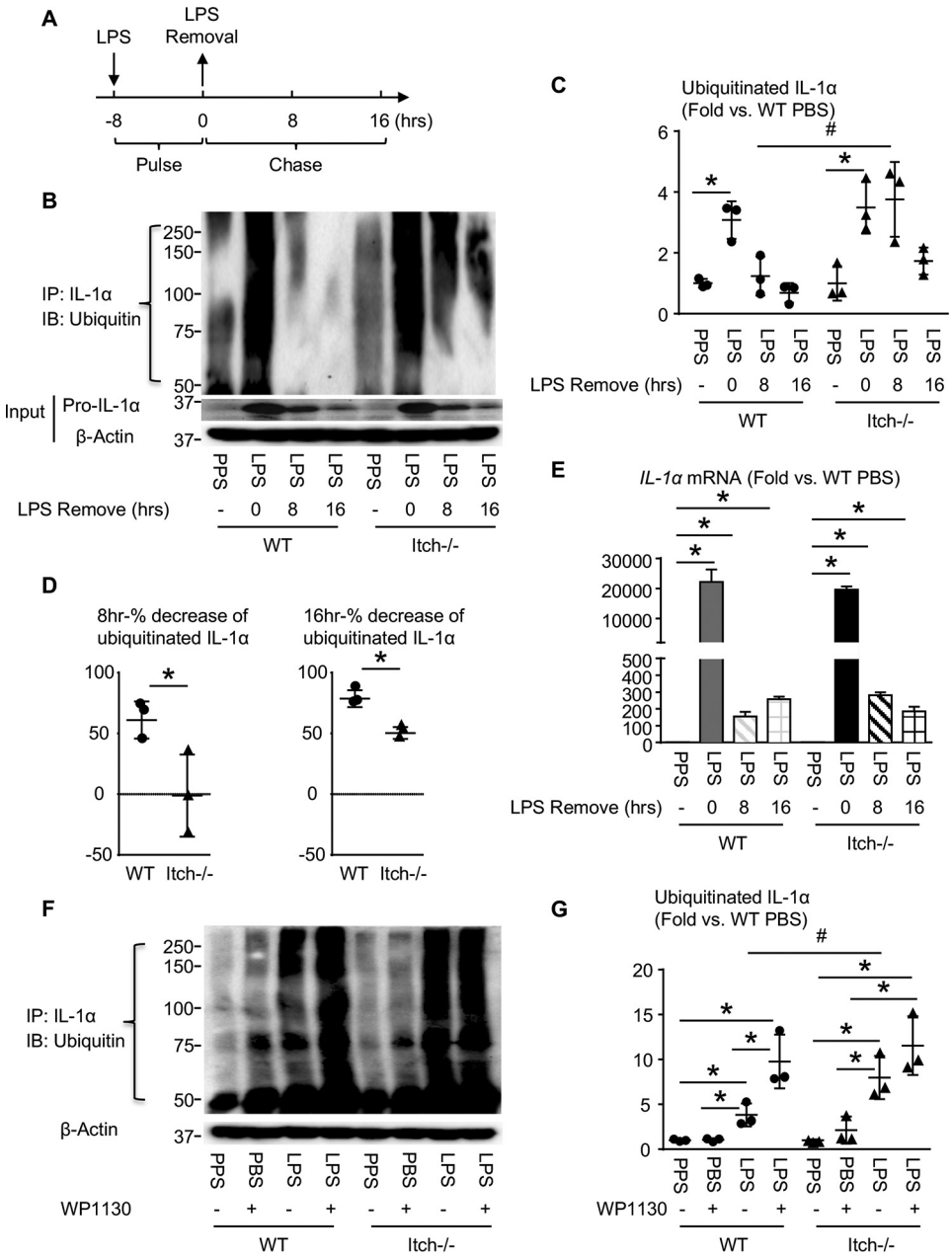

Figure 5. Deubiquitination of IL-1α decreases in Itch−/− pro-inflammatory macrophages. *A*, time course experimental design for *panels B–E*. BMMs from Itch−/− mice or WT littermate controls were induced with PBS/LPS (500 ng/ml), washed, and cultured in PBS to assess the deubiquitination of IL-1α for the indicated time. *B*, IL-1α was immunoprecipitated with anti–IL-1α antibodies and IP complexes were blotted with an anti-ubiquitin antibody. Ubiquitinated IL-1α decreased after 8 h of culture in PBS in WT macrophages, while still presented in Itch−/− macrophages. *C*, densitometry analysis was done similarly to Fig. 4. *D*, % decrease of ubiquitinated IL-1α 8 h or 16 h compared with macrophages before LPS removal after removing LPS was calculated. *E*, IL-1α mRNA levels from the same cells were measured by RT-qPCR, showing that the level of IL-1α decreased after removing LPS stimuli in the culture in both WT and Itch−/− cells. *F*, BMMs were treated with LPS for 8 h. After removing LPS from the culture media, macrophages were treated with nonselective DUB inhibitor WP1130 (1 μM) for 8 h IL-1α was IP with anti–IL-1α antibodies and IP complexes were blotted with an anti-ubiquitin antibody. Ubiquitinated IL-1α increased with WP1130 treatment, similar to Itch−/− macrophages after LPS induction. *G*, densitometry analysis was done similarly to Fig. 4. Data were analyzed with two-way ANOVA followed by Sidak's post hoc test. Values are mean ± S.D. of $n = 3$. *, $p <$ 0.05 LPS-macs *versus* PBS-macs; #, $p < 0.05$ Itch−/− cells *versus* WT cells (only the statistics of the comparison between Itch−/− *versus* WT with the same treatment are shown).

macs (-fold increase of over WT PBS-macs: 2.00 ± 0.45 in LPS-macs *versus* 1.00 ± 0.11 in PBS-macs in WT cells, 1.66 ± 0.38 in LPS-macs *versus* 1.05 ± 0.24 in PBS-macs in Itch−/− cells), there was no difference between WT and Itch−/− LPS-macs (-fold increase of LPS-macs over WT PBS-macs: 1.66 ± 0.38 in Itch−/− *versus* 2.00 ± 0.45 in WT cells) (Fig. 6*C*), suggesting that Itch's regulation of IL-1α maturation was independent of granzyme B. To further support that ITCH depletion promotes IL-1α maturation, we knocked down ITCH in WT macrophages using siRNA approach. Compared with control siRNA-transfected cells, cells that were transfected with siRNA *Itch* had 60% reduction in ITCH protein expression (-fold increase of ITCH in LPS-macs over control PBS-macs: 0.84 ± 0.04 in *Itch* siRNA *versus* 1.40 ± 0.20 in control siRNA) (Fig. 6*D*).

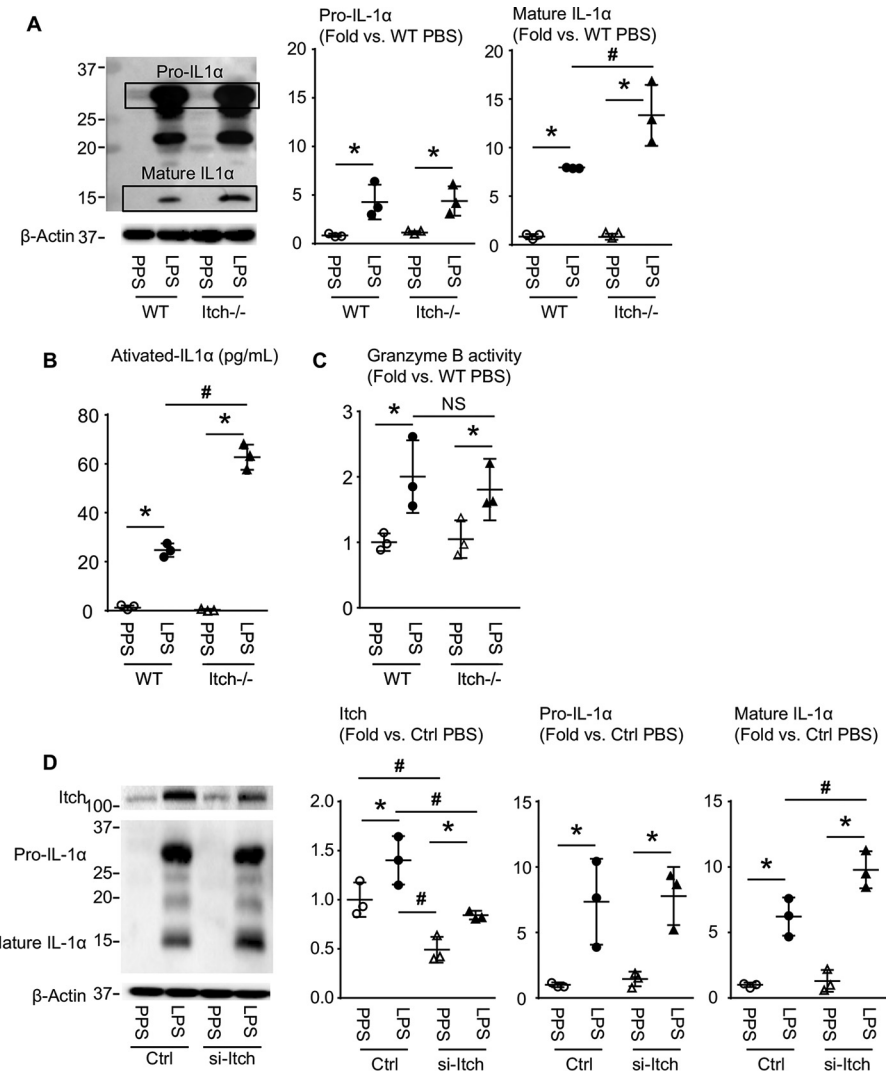

Figure 6. Increased mature form of IL-1α in Itch−/− pro-inflammatory macrophages. BMMs from Itch−/− mice or WT littermate controls were treated as in Fig. 3. *A*, pro form and mature form of IL-1α are distinguished using molecular weight in Western blot analysis (pro form: 31 kDa, activated form 17 kDa). Pro form IL-1α increased after LPS stimulation, with no difference between WT and Itch−/− macrophages. Mature form IL-1α was higher in Itch−/− LPS-macs compared with WT. *B*, secreted IL-1α in the supernatant was assessed with a ELISA kit, showing higher mature IL-1α in Itch−/− LPS-macs. *C*, granzyme B activity was assessed with specific fluorescent substrate acetyl-IETD-AFC (Ac-IETD-AFC). Production of AFC was monitored in a spectrofluorimeter and normalized to WT PBS-treated macrophages. *D*, si-Itch was used to knock down *Itch* in macrophages. ITCH protein level was assessed to evaluate the effectiveness of the knockdown. Pro form and mature form of IL-1α are distinguished using molecular weight in Western blot analysis. Densitometry analysis for Itch, pro and mature form of IL-1α. Data were analyzed with two-way ANOVA followed by Sidak's post hoc test. Values are mean ± S.D. of $n = 3$. *, $p < 0.05$ LPS-macs *versus* PBS-macs; #, $p < 0.05$ Itch−/− cells *versus* WT cells (only the statistics of the comparison between Itch−/− *versus* WT with the same treatment are shown).

Most importantly, *Itch* knockdown macrophages showed ~1.6-fold increase of mature IL-1α than control macrophages, a similar increase in Itch−/− cells over WT cells (-fold increase of LPS-macs over control PBS-macs: 9.78 ± 1.15 in *Itch* siRNA *versus* 6.21 ± 1.19 in control siRNA) (Fig. 6*D*). These data further indicate that ITCH inhibits IL-1α maturation by decreasing the maturation process of ubiquitinated IL-1α.

IL-1α neutralizing antibody partially inhibits pro-inflammatory polarization of Itch−/− macrophages

To further support the argument that IL-1α maturation contributes to susceptibility of Itch−/− macrophage to pro-inflammatory polarization, we examined whether IL-1α neutralizing antibodies (IL-1α–Ab) can rescue the increased pro-inflammatory phenotype in Itch−/− LPS-macs by immunofluorescence staining for iNOS intensity and qPCR analyzing for the expression of *NOS2*. IL-1α–Ab treatment slightly, about 35%, decreased iNOS intensity in WT cells (-fold increase of LPS- over PBS-macs: 3.30 ± 0.49 in IL-1α–Ab *versus* 5.03 ± 0.48 in IgG control, $p = 8.54 \times 10^{-5}$). More substantial, about 47%, decrease was observed in Itch−/− cells (-fold increase of LPS-macs over PBS-macs: 4.34 ± 058 in IL-1α–Ab *versus* 8.24 ± 0.50 in IgG control, $p = 3.26 \times 10^{-6}$) Fig. 7, *A* and *B*. An equivalent amount of IgG was used as control and did not affect iNOS signal intensity. IL-1α–Ab reduced the expression of *NOS2* mRNA by ~3-fold in Itch−/− LPS-macs (-fold increase of LPS-macs over WT PBS-macs: 3428.44 ± 236.35 in IL-1α–Ab *versus* 9182.04 ± 387.50 in IgG control, $p = 1.57 \times 10^{-5}$), but did not affect WT macrophages (-fold increase of LPS-macs over WT PBS-macs: 2991.97 ± 254.71 in IL-1α–Ab

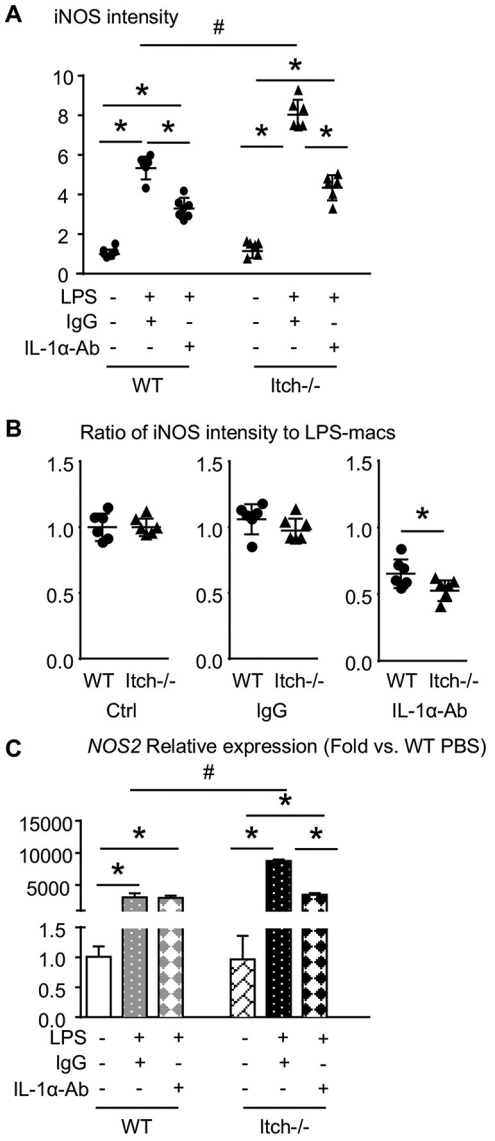

Figure 7. IL-1α neutralizing antibody partially inhibits inflammation in LPS induced Itch−/− macrophages. BMMs from Itch−/− mice or WT littermate controls were cultured as in Fig. 3 and were treated with PBS/LPS (500 ng/ml) ± IL-1α neutralizing antibody (IL-1α-Ab) (2 ug/ml) or IgG control. *A*, macrophages were immunofluorescence-stained cells for iNOS, a marker for pro-inflammatory macrophages. $n = 3$ repeats. iNOS intensity was quantified with ImageJ. Values are the mean ± S.D. of six wells. *B*, ratio of iNOS intensity after IgG or IL-1α-Ab treatment to nontreated LPS-macs. *C*, *NOS2* mRNA level is assessed with RT-qPCR showing IL-1α-Ab does not affect *NOS2* level in WT LPS-macs, but decreases *NOS2* level in Itch−/− LPS-macs. Data are analyzed with two-way ANOVA followed by Sidak's post hoc test. Values are mean ± S.D. of $n = 6$. *, $p < 0.05$ LPS-macs *versus* PBS-macs; #, $p < 0.05$ Itch−/− cells *versus* WT cells (only the statistics of the comparison between Itch−/− *versus* WT with the same treatment are shown).

versus 3616.50 ± 82.99 in IgG control, $p = 0.87$) (Fig. 7*C*). These data suggest that increased activated IL-1α is correlated with increased susceptibility of macrophage polarization in Itch−/− macrophages.

Discussion

Recent studies demonstrated the importance of mac polarization in various pathological conditions, which are controlled by intricate signaling pathway crosstalk. Using ubiquitin proteomics, we showed that the ub profiles are distinct in polarized macrophages. We also found that the ub status of IL-1α is associated with its maturation, which is mediated by ubiquitin E3 ligase ITCH. ITCH depletion in macrophages resulted in elevated ubiquitinated IL-1α, decreased IL-1α de-ub, increased mature IL-1α, and more severe pro-inflammatory polarization (Fig. 8). This implies that modulating ub of key proteins may be a viable approach to manipulate macrophage phenotype and interfere with macrophage-mediated diseases.

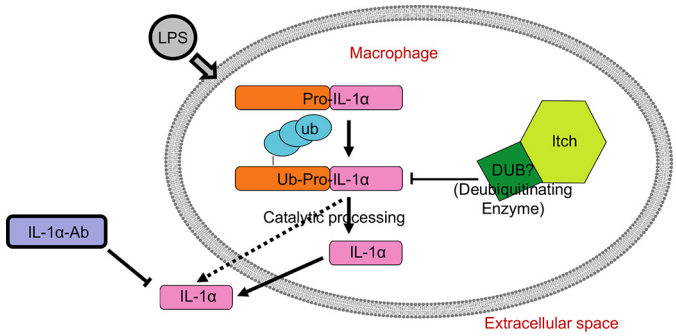

Figure 8. ITCH negatively regulates inflammation by reducing ubiquitinated IL-1α and IL-1α maturation. LPS stimulation can induce the transcription of pro–IL-1α, which is then ubiquitinated for catalytic processing to mature IL-1α, which has increased bioactivity and solubility. The ub of IL-1α is reversed by DUB complex where ITCH functions as an adaptor protein.

Previous studies linked protein ub with macrophage polarization. E3 ligases TRAF6 (22), Pellino1 (23), and Praja2 (24) catalyze the Lys-63–ub to activate positive regulators of NF-κB and JunB pathways in macrophages to promote pro-inflammatory polarization. In contrast, E3 ligase Cbl-b inhibits mac pro-inflammatory polarization by catalyzing the ub of Toll-like receptor 4 for its degradation (25). In this study, we demonstrate that ITCH regulates mac polarization by modulating the ub of pro-inflammatory cytokine IL-1α. These findings suggest that the ub status of specific proteins in macrophages may result in opposite outcomes on their polarization, *e.g.* negative regulators of inflammation are ubiquitinated for degradation, whereas positive regulators are ubiquitinated for activation.

Using ub proteomics, we reported for the first time that ub profiles of PBS-, LPS-, or IL-4–treated macrophages are different. Specific ubiquitinated proteins in PBS-macs and IL-4–macs involved in a wide range of housekeeping proteins such as RNA transcription (26, 27), posttranslational modification (28–30), mitochondria function (31, 32), glutamate metabolism (33), intracellular trafficking (34, 35), and so on. More interestingly, cellular structural proteins including actin-related protein 10 are specifically ubiquitinated in IL-4–macs, which might be related to the shift to elongated shape during anti-inflammatory macrophage polarization (36). In contrast, among the top eight specifically ubiquitinated proteins identified in LPS-macs (Fig. 2*C*, and Table 1), seven are known regulators of inflammation, including IL-1α and iNOS. Suppressor of cytokine signaling 2 (SOCS3) is a negative regulator of cytokine signaling by functioning as a part of a multi-subunit E3 ligase complex (37). The substrates of SOCS3 include important inflammatory regulators such as TRAF6, Janus kinase, and insulin receptor substrate 1/2 (37, 38). Interferon-induced GTP-binding protein Mx1/Mx2, C-type lectin, and serum

amyloid A3 protein are critical for host anti-viral (39), anti-bacteria (40), and acute inflammatory (41) responses, respectively. However, the effects of ub on the function of these inflammatory regulators during mac polarization are unclear, which warrants future investigation.

We demonstrated that the ub of IL-1α is important for its processing to the mature form, which raises three questions that warrant further investigations. First, although we showed that ITCH indirectly facilitated IL-1α maturation, we did not explore what proteases and cellular compartments are involved in ubiquitinated IL-1α cleavage. Multiple proteases, including neutrophil elastase, granzyme B, cathepsin G, and proteinase-3, have been reported to cleave pro–IL-1α at different amino acid residues (21). Thus, whether ITCH also affects the level or activity of IL-1α processing proteases needs to be explored in the future. Second, the location of IL-1α proteolytic processing can be intracellular or extracellular, depending on the protease (13). We showed that increased secreted soluble IL-1α in the supernatant of Itch−/− LPS-macs is correlated with more severe inflammation, which can be partially reversed with IL-1α neutralization, suggesting that IL-1α is processed intracellularly and secreted as a mature form. However, it is also possible that ubiquitinated IL-1α is secreted to the extracellular space and exposed to the proteases in the interstitial space. Third, the effects of IL-1α maturation are unclear. Unlike IL-1β, another member in the IL-1 cytokine family whose biological function depends on its catalytic processing and maturation, both pro–IL-1α and mature IL-1α bind to IL1R with comparable kinetics *in vitro* (42, 43), suggesting that the maturation might not be necessary for IL-1α bioactivity. However, Afonina *et al.* (21) reported that the bioactivity of mature IL-1α is several times higher than the pro form *in vivo*. Watanabe and Kobayashi (44) also reported that catalytic processing of IL-1α to mature form promotes the secretion of IL-1α. Increased *in vivo* bioactivity of mature IL-1α may be related to the solubility of mature IL-1α, which facilitates its dissemination to exert systemic effects, compared with the membrane-bound pro–IL-1α. Furthermore, pro–IL-1α is subjected to intracellular proteasomal degradation (19), which might be protected from the maturation process. We showed that increased secreted IL-1α is correlated with increased inflammation in Itch−/− macrophages and can be partially reversed by an IL-1α neutralizing Ab, supporting the argument that maturation of IL-1α increases its bioactivity.

We found that ITCH regulates IL-1α ub by promoting its de-ub. De-ub is a process to remove ubiquitin from proteins and other molecules, which is carried out by DUB. Recent studies demonstrate the important role of DUBs in controlling inflammation. DUB A20 (11) and CYLD (12) negatively regulate NF-κB signaling pathway in macrophages by removing the Lys-63–ub on TRAF6. Mice deficient for A20 or CYLD develop chronic inflammatory phenotype. ITCH is a ubiquitin E3 ligase. ITCH catalyzes the Lys-48–ub of the pro-inflammatory AP-1 and JunB transcription factors, marking them for degradation, and consequently inhibits the expression of downstream cytokines in T cells (10). In contrast, ITCH forms complexes with DUB enzymes A20 (11) or CYLD (12) to reverse the Lys-63–ub of TRAF6 and down-regulate the NF-κB pathway in macrophages. Our findings of the involvement of ITCH in IL-1α de-ub and maturation reveal a new molecular mechanism for inhibitory role of ITCH in inflammation.

Pro-inflammatory stimuli culminate in the activation of a few key signaling pathways (*e.g.* NF-κB), resulting in similar transcriptional changes in macrophages. However, different levels or combinations of stimuli lead to a complex continuum spectrum of phenotypes instead of the simplified M1-M2 paradigm, and markers for polarized macrophage populations are not well-defined (2, 45). In the current study, we used iNOS as an *in vitro* marker for pro-inflammatory macrophages. It is known that iNOS which, in addition to its bactericidal functions, mediates various inflammatory diseases such as posttraumatic osteoarthritis (15). However, iNOS alone is not a reliable marker for mac polarization *in vivo*. Therefore, we recognize the limitation of using iNOS as a single marker for LPS macrophages. Characterizing specific panels of markers of polarized macrophage population in future *in vivo* studies is necessary.

Conclusion

We showed that the ub of specific proteins in inflammatory pathways alter macrophage polarization. Specifically, the de-ub of IL-1α regulated by ITCH inhibits pro-inflammatory macrophage polarization by blocking pro–IL-1α maturation. Based on our findings, it is beneficial to modulate the ub of specific proteins to alter the macrophage phenotype as a treatment for inflammatory diseases.

Materials and methods

Animals and cell cultures

Itch−/− mice (3–6 months, male and female) were generated previously on a C57BL/6J background and were genotyped by PCR analysis (12), and WT littermates were used as controls. Bone marrow (BM) cells were flushed from femurs and tibias and cultured with conditioned medium (1:50 dilution) from a macrophage colony-stimulating factor–producing cell line (46) for 3 days in α-MEM with 10% FBS (Gibco 26140-079) to generate BM macrophages (BMMs). BMMs were treated with LPS (Sigma-Aldrich, L4391; 100 ng/ml or 500 ng/ml) (LPS-macs) or IL-4 (R&D Systems, 404-ML-010; 100 ng/ml) (IL-4–macs) for further experiments as described below. PBS-treated WT macrophages (WT PBS-macs) were used as controls. All animal use in this study has been approved by the Animal Care and Use Committee at the University of Rochester.

Quantitative Real-Time PCR

Total RNA was extracted using TRIzol reagent (Invitrogen). cDNAs were synthesized using the iSCRIPT cDNA Synthesis Kit (Bio-Rad, 1708891). Quantitative real-time PCR (qPCR) amplifications were performed in the iCycler (Bio-Rad) real-time PCR machine using the iQ SYBR Green Supermix (Bio-Rad, 1808882) according to the manufacturer's instructions. Actin was amplified on the same plates and used to normalize the data. Each sample was prepared in triplicate, and each experiment was repeated at least three times. -Fold changes of genes of interest were calculated by normalizing to PBS-treated WT macrophages

Table 2
List of primers used in the real-time polymerase chain reaction

Genes	Sequences of primers	GenBank accession number	Locus on gene	Product size (bp)
IL1β	F: 5′ GACTTCACCATGGAATCCGT 3′ R: 5′ CCATGGTTTCTTGTGACCCT 3′	NM_008361	868-1039	172
NOS2	F: 5′ AACGGAGAACGTTGGATTTG 3′ R: 5′ CAGCACAAGGGGTTTTCTTC 3′	NM_010927	212-358	147
TNF	F: 5′ CACACTCAGATCATCTTCTCAA 3′ R: 5′ AGTAGACAAGGTACAACCCATC 3′	NM_013693	401-582	182
IL10	F: 5′ CTATCCCTTGATGCCATTACCAG 3′ R: 5′ ATCCACATGGTTGGGAAGTTC 3′	NM_008607.2	906-1049	144
β-actin	F: 5′ GTCAGGATCTTCATGAGGTAGT 3′ R: 5′ ACCCAGATCATGTTTGAGAC 3′	NM_007393	280-503	224

as 1. The sequences of primer pairs for *IL1β*, *NOS2*, *TNF*, *IL10*, *PPAR*, *IL1α*, and *actin* mRNAs are shown in Table 2.

Immunofluorescence staining

Cells cultured in 96-well plates were fixed with 10% formalin for immunofluorescence staining. Briefly, cells were blocked with 5% normal donkey serum (Jackson ImmunoResearch Laboratories, 017-000-121, diluted in PBS with 0.1% Triton X) for 30 min at room temperature. Cells were incubated with primary antibodies iNOS (Santa Biotechnology, sc-650, 1:200) or CD206 (R&D Systems, AF2535, 1:100) at 4°C overnight, followed by secondary antibodies goat anti-rabbit Alexa Fluor 488 (Abcam, ab150077, 1:500) and rabbit anti-goat Alexa Fluor 568 (Thermo Fisher, A21085, 1:400) at room temperature for 1 h, and finally stained with 4′,6-diamidino-2-phenylindole (DAPI, 1 μg/ml) for 10 min. Antibodies were diluted in 1% normal donkey serum (diluted in PBS with 0.1% Triton X). Cells were imaged with an Olympus 1 × 71 microscope at 20× magnification. To quantify iNOS+ cells, ImageJ was used to calculate the intensity density of F4/80+ staining. For the quantification of iNOS staining in the 96-well, one image was taken for each well under 10× magnification was imported to the ImageJ software, with a total of three wells for each group. Thresholds were determined for positive and negative staining and maintained the same throughout analysis. Percentage of iNOS+ area was measured using the "Area Fraction" modality.

LC–MS (LC–MS/MS) for ubiquitinated proteins

Primary BMMs pooled from five C57Bl/6 mice were cultured to induce PBS-, LPS-, or IL-4–macs as described above and were collected for ubiquitin proteomics following a published protocol (18). In brief, cells were lysed in freshly prepared urea lysis buffer. Protein concentration was measured using the Pierce BCA protein assay kit (Thermo Fisher, cat. no. 23225). Disulfide bonds were reduced with 2 mM DTT for 1 h at room temperature. Cysteine residues were carbamidomethylated by adding 10 mM iodoacetamide for 30 min incubation at room temperature in the dark. Proteins were precipitated using the chloroform/methanol precipitation method, followed by resuspension in 1 M urea, 50 mM HEPES. Enzymatic digestion was performed using trypsin (Pierce) at a 1:50 enzyme:protein ratio overnight at 37°C. The reaction was quenched in the morning by the addition of formic acid (Pierce) to 1%. The peptide solution was centrifuged for 5 min at 10,000 × *g* to remove precipitates. Peptides were desalted using a 130-mg C18 SepPak cartridge (Waters) and then dried down in a Centrivap Concentrator (Labconco).

For immunoaffinity purification of K-ϵ-GG peptides, lyophilized peptides were reconstituted, and ubiquitin-modified peptides were enriched with PTMScan ubiquitin remnant motif (K-ϵ-GG) kit (Cell Signaling Technology, cat. no. 5562). In brief, reconstituted peptides were incubated with K-ϵ-GG–specific antibody cross-inked Protein-A agarose beads, and eluted with IAP elution buffer (50 mM MOPS, pH 7.2, 10 mM sodium phosphate and 50 mM NaCl, 0.15% (v/v) TFA). Then peptides were desalted with a homemade C18 column.

For LC–MS/MS, K-ϵ-GG–enriched samples were reconstituted in 20 μl TFA (0.1%, JT Baker) and 6 μl (30%) was loaded onto a homemade 30-cm C18 column, with 1.8 μM beads (Sepax) using an Easy nLC-1000 (Thermo Scientific). The mobile phases were 0.1% formic acid in water (JT Baker) and 0.1% formic acid in acetonitrile (JT Baker). The gradient began at 3% B, went to 8% over 5 min, to 30% over 68 min, then to 70% B in 4 min and was held there for 4 min. The gradient was returned to initial conditions in 3 min and the column was allowed to re-equilibrate for 10 min. The flow rate was kept constant at 300 nl/min. The peptides were detected using a Q Exactive Plus mass spectrometer (Thermo Scientific), using a data-dependent top 10 method. A full scan from 400–1400 m/z was collected at 70,000 resolution with a maximum ion injection time of 50 ms, and an AGC setting of 1×10^6. The MS2 spectra were collected at 17,500 resolution using a normalized collision energy of 27, an isolation width of 1.5 Da, a maximum ion injection time of 200 ms, and an AGC setting of 5×10^4. Dynamic exclusion was enabled and set at 25 s, with a repeat count of 1.

MS data analysis

MS data were searched using the Mascot search engine (Matrix Science) within the Proteome Discoverer software platform, version 2.2 (Thermo Fisher), using the SwissProt *Mus musculus* database. Percolator was used as the false discovery rate calculator, filtering out peptides that had q-values greater than 0.01. To semi-quantify the protein relative abundance in multiple samples, the peak area of the extracted ion chromatograms for each peptide precursor in the full scan was calculated using the Minora Feature Detector node within Proteome Discoverer, which also used retention time alignment and precursor mass to link peptides across runs, which reduces the level of missing values. The abundance of an individual protein was calculated as the sum of its peak areas for all peptides derived from that protein. The relative concentration of each protein

was determined by comparing the total MS intensities of all identified peptides from that protein in one sample *versus* those from other samples. Raw dataset of MS was uploaded to PRIDE (identifier PXD018743). Proteins with an abundance above 1×10^7 and at least two identified unique peptides that were specifically ubiquitinated in each condition were identified in Table 2. A list of all ubiquitinated proteins with peptide sequences with diglycine tags was included in Table S1.

Western blot analysis

Cells were lysed in ub-lysis buffer containing 1 × RIPA buffer (EMD Millipore, 20-188), 1 mM DTT (Sigma-Aldrich), 1 mM PMSF (Sigma-Aldrich), and 5 mM *N*-ethylmaleimide (Millipore Sigma, 10197777001). To determine the total ub level, proteins were loaded onto 8% SDS-PAGE gel, and blotted with anti-ubiquitin Ab (Santa Cruz Biotechnology, sc-8017, 1:200). For pro–IL-1α and activated-IL-1α level, proteins were loaded onto 12% SDS-PAGE gel and incubated with anti–IL-1α Ab (R&D Systems, AF-400-NA, 1:500). The pro form and mature form of IL-1α were distinguished by molecular weight: 31 kDa and 17 kDa, respectively (19). β-actin (Sigma-Aldrich, 1:5000) was used as a loading control. ImageJ was used to quantify pro and mature IL-1α, normalized to β-actin, and then normalized to PBS-treated WT macrophages.

Immunoprecipitation

Cells were lysed in ub-lysis buffer and subjected to immunoprecipitation (IP) as described before (12). Briefly, 500 μg of proteins were diluted in 100 μl ub-lysis buffer and mixed with 1 μg of antibodies (iNOS and IL-1α), incubated for 1 h at 4°C, and then incubated with prewashed EZview Red Protein A/G Affinity Gel beads (Millipore Sigma, P6486/E3403) overnight at 4°C. The bound antigens were eluted from the beads by boiling in the eluting buffer for 5 min. Eluted samples were fractionated by 8% SDS-PAGE gel and incubated with anti-ubiquitin antibody (Santa Cruz Biotechnology, sc-8017, 1:200).

Deubiquitination assay

BMMs were induced with LPS (500 ng/ml) or PBS control for 8 h. Then cells were washed with PBS and treated with 1 μM *N*-ethylmaleimide and harvested 8 h or 16 h after removing LPS. Cells were harvested for IP and RT-qPCR as described above.

ELISA

Secreted IL-1α was measured with ELISA. Briefly, secreted IL-1α in 50 μl of freshly collected supernatant was assessed using the mouse IL-1α/IL-1F1 quantikine ELISA kit (R&D System, MLA00) following the manufacturer's instructions.

Granzyme B activity

Whole cell lysate was harvested for granzyme B and caspase activity measurement. Briefly, 100 μg of whole cell lysate was added to caspase assay buffer (Enzo, BML-Kl111-0020) containing 50 μM of fluorogenic Ac-IETD-AFC fluorogenic peptide substrates (Enzo, ALX-260-110-M005) and incubated at 37°C for 1 h. Production of AFC was monitored in a spectrofluorimeter with an excitation wavelength of 400 nm and an emission wavelength of 505 nm. The results were presented as the -fold change *versus* the WT PBS-macs.

siRNA transfection to deplete Itch in WT macrophages

Murine *Itch* siRNA (4390771 assay ID s68414) and BLOCK-iT Alexa Fluor red fluorescent control siRNA (Thermo Fisher, 14750100) were purchased from Thermo Fisher Silencer Select website. The siRNA transfection was performed following the manufacturer's instructions. In brief, BMMs from WT mice at 60% confluence were transfected with 10 μM *Itch* siRNA and control siRNA diluted in lipofectamine RNAiMAX Reagent (Thermo Fisher, 13778030) for 2 days. Cells were then treated with LPS to induce LPS-macs. Whole cell lysates were harvested for Western blot analysis. The transfection efficacy in cells treated with control siRNA was 87.96% ± 6.29%. The *Itch* knock-down was determined by Western blotting.

Statistical analysis

Statistical analyses were performed using Prism7 software. Data are presented as mean ± S.D. One-way analysis of variance followed by Tukey post hoc test was used to compare PBS-, LPS-, and IL-4–treated WT macrophages. Two-way analysis of variance followed by Sidak's post hoc test was used to compare WT or Itch−/− macrophages with different treatments. *p*-values less than or equal to 0.05 were considered significant.

Data availability

The MS dataset is uploaded to PRIDE, accessible at PXD018743.

Acknowledgments—We thank Dr. Sina Ghaemmaghami and Kevin Welle in the Mass Spectrometry Resource Laboratory, University of Rochester Medical Center, for preparing method description of mass spectrometry and for helping on data upload.

Author contributions—X. L., H. Z., B. F. B., and L. X. conceptualization; X. L., H. Z., and L. X. data curation; X. L. and L. X. software; X. L., H. Z., B. F. B., and L. X. formal analysis; X. L. validation; X. L. and L. X. investigation; X. L. visualization; X. L., H. Z., and L. X. methodology; X. L. writing-original draft; X. L. and L. X. project administration; X. L., B. F. B., and L. X. writing-review and editing; B. F. B. and L. X. supervision; L. X. resources; L. X. funding acquisition.

Funding and additional information—This work was supported by NIAMS, National Institutes of Health Research Grants AR059775, AR069789, and AR049994 (to L. X.) from the United States Public Service. The content is solely the responsibility of the authors and does not necessarily represent the official views of the National Institutes of Health.

Conflict of interest—The authors declare that they have no conflicts of interest with the contents of this article.

Abbreviations—The abbreviations used are: mac, macrophage; TNF, tumor necrosis factor; LPS, lipopolysaccharide; iNOS, inducible NOS;

ub, ubiquitination; de-ub, deubiquitination; DUB, de-ub enzymes; BMM, bone marrow macrophage; qPCR, quantitative real-time PCR; IP, immunoprecipitation; ANOVA, analysis of variance.

References

1. Editorial. (2017) A current view on inflammation. *Nat. Immunol.* **18,** 825 CrossRef Medline
2. Hamidzadeh, K., Christensen, S. M., Dalby, E., Chandrasekaran, P., and Mosser, D. M. (2017) Macrophages and the recovery from acute and chronic inflammation. *Ann. Rev. Physiol.* **79,** 567–592 CrossRef Medline
3. Mills, C. D., Kincaid, K., Alt, J. M., Heilman, M. J., and Hill, A. M. (2000) M-1/M-2 macrophages and the Th1/Th2 paradigm. *J. Immunol.* **164,** 6166–6173 CrossRef Medline
4. Sica, A., and Mantovani, A. (2012) Macrophage plasticity and polarization: In vivo veritas. *J. Clin. Invest.* **122,** 787–795 CrossRef Medline
5. Orecchioni, M., Ghosheh, Y., Pramod, A. B., and Ley, K. (2019) Macrophage polarization: Different gene signatures in M1(LPS+) vs. classically and M2 (LPS−) vs. alternatively activated macrophages. *Front. Immunol.* **10,** 1084 CrossRef Medline
6. Bhoj, V. G., and Chen, Z. J. (2009) Ubiquitylation in innate and adaptive immunity. *Nature* **458,** 430–437 CrossRef Medline
7. Chen, Z., Hagler, J., Palombella, V. J., Melandri, F., Scherer, D., Ballard, D., and Maniatis, T. (1995) Signal-induced site-specific phosphorylation targets IκBα to the ubiquitin-proteasome pathway. *Genes Dev.* **9,** 1586–1597 CrossRef Medline
8. Wang, C., Deng, L., Hong, M., Akkaraju, G. R., Inoue, J., and Chen, Z. J. (2001) TAK1 is a ubiquitin-dependent kinase of MKK and IKK. *Nature* **412,** 346–351 CrossRef Medline
9. Aki, D., Zhang, W., and Liu, Y. C. (2015) The E3 ligase Itch in immune regulation and beyond. *Immunol. Rev.* **266,** 6–26 CrossRef Medline
10. Gao, M., Labuda, T., Xia, Y., Gallagher, E., Fang, D., Liu, Y. C., and Karin, M. (2004) Jun turnover is controlled through JNK-dependent phosphorylation of the E3 ligase Itch. *Science* **306,** 271–275 CrossRef Medline
11. Shembade, N., Harhaj, N. S., Parvatiyar, K., Copeland, N. G., Jenkins, N. A., Matesic, L. E., and Harhaj, E. W. (2008) The E3 ligase Itch negatively regulates inflammatory signaling pathways by controlling the function of the ubiquitin-editing enzyme A20. *Nat. Immunol.* **9,** 254–262 CrossRef Medline
12. Zhang, H., Wu, C., Matesic, L. E., Li, X., Wang, Z., Boyce, B. F., and Xing, L. (2013) Ubiquitin E3 ligase Itch negatively regulates osteoclast formation by promoting deubiquitination of tumor necrosis factor (TNF) receptor-associated factor 6. *J. Biol. Chem.* **288,** 22359–22368 CrossRef Medline
13. Malik, A., and Kanneganti, T. D. (2018) Function and regulation of IL-1α in inflammatory diseases and cancer. *Immunol. Rev.* **281,** 124–137 CrossRef Medline
14. Duong, B. H., Onizawa, M., Oses-Prieto, J. A., Advincula, R., Burlingame, A., Malynn, B. A., and Ma, A. (2015) A20 restricts ubiquitination of pro-interleukin-1β protein complexes and suppresses NLRP3 inflammasome activity. *Immunity* **42,** 55–67 CrossRef Medline
15. Wang, W., Lin, X., Xu, H., Sun, W., Bouta, E. M., Zuscik, M. J., Chen, D., Schwarz, E. M., and Xing, L. (2019) Attenuated joint tissue damage associated with improved synovial lymphatic function following treatment with bortezomib in a mouse model of experimental posttraumatic osteoarthritis. *Arthritis Rheumatol.* **71,** 244–257 CrossRef Medline
16. Sun, W., Zhang, H., Wang, H., Chiu, Y. G., Wang, M., Ritchlin, C. T., Kiernan, A., Boyce, B. F., and Xing, L. (2017) Targeting notch-activated m1 macrophages attenuates joint tissue damage in a mouse model of inflammatory arthritis. *J. Bone Miner. Res.* **32,** 1469–1480 CrossRef Medline
17. Smith, T. D., Tse, M. J., Read, E. L., and Liu, W. F. (2016) Regulation of macrophage polarization and plasticity by complex activation signals. *Integr. Biol. (Camb)* **8,** 946–955 CrossRef Medline
18. Udeshi, N. D., Mertins, P., Svinkina, T., and Carr, S. A. (2013) Large-scale identification of ubiquitination sites by mass spectrometry. *Nat. Protoc.* **8,** 1950–1960 CrossRef Medline
19. Ainscough, J. S., Frank Gerberick, G., Zahedi-Nejad, M., Lopez-Castejon, G., Brough, D., Kimber, I., and Dearman, R. J. (2014) Dendritic cell IL-1α and IL-1β are polyubiquitinated and degraded by the proteasome. *J. Biol. Chem.* **289,** 35582–35592 CrossRef Medline
20. Kolodziejski, P. J., Musial, A., Koo, J. S., and Eissa, N. T. (2002) Ubiquitination of inducible nitric oxide synthase is required for its degradation. *Proc. Natl. Acad. Sci. U.S.A.* **99,** 12315–12320 CrossRef Medline
21. Afonina, I. S., Tynan, G. A., Logue, S. E., Cullen, S. P., Bots, M., Lüthi, A. U., Reeves, E. P., McElvaney, N. G., Medema, J. P., Lavelle, E. C., and Martin, S. J. (2011) Granzyme B-dependent proteolysis acts as a switch to enhance the proinflammatory activity of IL-1α. *Mol. Cell* **44,** 265–278 CrossRef Medline
22. Deng, L., Wang, C., Spencer, E., Yang, L., Braun, A., You, J., Slaughter, C., Pickart, C., and Chen, Z. J. (2000) Activation of the IκB kinase complex by TRAF6 requires a dimeric ubiquitin-conjugating enzyme complex and a unique polyubiquitin chain. *Cell* **103,** 351–361 CrossRef Medline
23. Murphy, M., Xiong, Y., Pattabiraman, G., Qiu, F., and Medvedev, A. E. (2015) Pellino-1 positively regulates Toll-like receptor (TLR) 2 and TLR4 signaling and is suppressed upon induction of endotoxin tolerance. *J. Biol. Chem.* **290,** 19218–19232 CrossRef Medline
24. Zhong, J., Wang, H., Chen, W., Sun, Z., Chen, J., Xu, Y., Weng, M., Shi, Q., Ma, D., and Miao, C. (2017) Ubiquitylation of MFHAS1 by the ubiquitin ligase praja2 promotes M1 macrophage polarization by activating JNK and p38 pathways. *Cell Death Dis.* **8,** e2763 CrossRef Medline
25. Abe, T., Hirasaka, K., Kagawa, S., Kohno, S., Ochi, A., Utsunomiya, K., Sakai, A., Ohno, A., Teshima-Kondo, S., Okumura, Y., Oarada, M., Maekawa, Y., Terao, J., Mills, E. M., and Nikawa, T. (2013) Cbl-b is a critical regulator of macrophage activation associated with obesity-induced insulin resistance in mice. *Diabetes* **62,** 1957–1969 CrossRef Medline
26. Visconti, R., Palazzo, L., Della Monica, R., and Grieco, D. (2012) Fcp1-dependent dephosphorylation is required for M-phase-promoting factor inactivation at mitosis exit. *Nat. Commun.* **3,** 894 CrossRef Medline
27. Odintsova, T. I., Müller, E. C., Ivanov, A. V., Egorov, T. A., Bienert, R., Vladimirov, S. N., Kostka, S., Otto, A., Wittmann-Liebold, B., and Karpova, G. G. (2003) Characterization and analysis of posttranslational modifications of the human large cytoplasmic ribosomal subunit proteins by mass spectrometry and Edman sequencing. *J Protein Chem.* **22,** 249–258 CrossRef Medline
28. Yang, Q., Co, D., Sommercorn, J., and Tonks, N. K. (1993) Cloning and expression of PTP-PEST. A novel, human, nontransmembrane protein tyrosine phosphatase. *J. Biol. Chem.* **268,** 6622–6628 CrossRef Medline
29. Krakow, D., Sebald, E., King, L. M., and Cohn, D. H. (2001) Identification of human FEM1A, the ortholog of a *C. elegans* sex-differentiation gene. *Gene* **279,** 213–219 CrossRef Medline
30. Shimizu, K., Tani, M., Watanabe, H., Nagamachi, Y., Niinaka, Y., Shiroishi, T., Ohwada, S., Raz, A., and Yokota, J. (1999) The autocrine motility factor receptor gene encodes a novel type of seven transmembrane protein. *FEBS Lett.* **456,** 295–300 CrossRef Medline
31. Santel, A., and Fuller, M. T. (2001) Control of mitochondrial morphology by a human mitofusin. *J. Cell Sci.* **114,** 867–874 CrossRef Medline
32. Brix, J., Ziegler, G. A., Dietmeier, K., Schneider-Mergener, J., Schulz, G. E., and Pfanner, N. (2000) The mitochondrial import receptor Tom70: Identification of a 25 kDa core domain with a specific binding site for preproteins. *J. Mol. Biol.* **303,** 479–488 CrossRef Medline
33. Rumping, L., Büttner, B., Maier, O., Rehmann, H., Lequin, M., Schlump, J. U., Schmitt, B., Schiebergen-Bronkhorst, B., Prinsen, H., Losa, M., Fingerhut, R., Lemke, J. R., Zwartkruis, F. J. T., Houwen, R. H. J., Jans, J. J. M., *et al.* (2019) Identification of a loss-of-function mutation in the context of glutaminase deficiency and neonatal epileptic encephalopathy. *JAMA Neurol.* **76,** 342–350 CrossRef Medline
34. Graves, A. R., Curran, P. K., Smith, C. L., and Mindell, J. A. (2008) The Cl-/H+ antiporter ClC-7 is the primary chloride permeation pathway in lysosomes. *Nature* **453,** 788–792 CrossRef Medline
35. Whitley, P., Hinz, S., and Doughty, J. (2009) Arabidopsis FAB1/PIKfyve proteins are essential for development of viable pollen. *Plant Physiol.* **151,** 1812–1822 CrossRef Medline
36. McWhorter, F. Y., Wang, T., Nguyen, P., Chung, T., and Liu, W. F. (2013) Modulation of macrophage phenotype by cell shape. *Proc. Natl. Acad. Sci. U.S.A.* **110,** 17253–17258 CrossRef Medline
37. Williams, J. J., Munro, K. M., and Palmer, T. M. (2014) Role of ubiquitylation in controlling suppressor of cytokine signalling 3 (SOCS3) function and expression. *Cells* **3,** 546–562 CrossRef Medline

38. Frobøse, H., Rønn, S. G., Heding, P. E., Mendoza, H., Cohen, P., Mandrup-Poulsen, T., and Billestrup, N. (2006) Suppressor of cytokine signaling-3 inhibits interleukin-1 signaling by targeting the TRAF-6/TAK1 complex. *Mol. Endocrinol.* **20,** 1587–1596 CrossRef Medline
39. Pilla-Moffett, D., Barber, M. F., Taylor, G. A., and Coers, J. (2016) Interferon-inducible GTPases in host resistance, inflammation and disease. *J. Mol. Biol.* **428,** 3495–3513 CrossRef Medline
40. Miyake, Y., Toyonaga, K., Mori, D., Kakuta, S., Hoshino, Y., Oyamada, A., Yamada, H., Ono, K., Suyama, M., Iwakura, Y., Yoshikai, Y., and Yamasaki, S. (2013) C-type lectin MCL is an FcRγ-coupled receptor that mediates the adjuvanticity of mycobacterial cord factor. *Immunity* **38,** 1050–1062 CrossRef Medline
41. De Buck, M., Gouwy, M., Wang, J. M., Van Snick, J., Proost, P., Struyf, S., and Van Damme, J. (2016) The cytokine-serum amyloid A-chemokine network. *Cytokine Growth Factor Rev.* **30,** 55–69 CrossRef Medline
42. Mosley, B., Urdal, D. L., Prickett, K. S., Larsen, A., Cosman, D., Conlon, P. J., Gillis, S., and Dower, S. K. (1987) The interleukin-1 receptor binds the human interleukin-1α precursor but not the interleukin-1β precursor. *J. Biol. Chem.* **262,** 2941–2944 Medline
43. Afonina, I. S., Müller, C., Martin, S. J., and Beyaert, R. (2015) Proteolytic processing of interleukin-1 family cytokines: Variations on a common theme. *Immunity* **42,** 991–1004 CrossRef Medline
44. Watanabe, N., and Kobayashi, Y. (1994) Selective release of a processed form of interleukin 1α. *Cytokine* **6,** 597–601 CrossRef Medline
45. Martinez, F. O., and Gordon, S. (2014) The M1 and M2 paradigm of macrophage activation: Time for reassessment. *F1000Prime Rep.* **6,** 13 CrossRef Medline
46. Takeshita, S., Kaji, K., and Kudo, A. (2000) Identification and characterization of the new osteoclast progenitor with macrophage phenotypes being able to differentiate into mature osteoclasts. *J. Bone Miner. Res.* **15,** 1477–1488 CrossRef Medline